Stabilization of S3O4 at High Pressure-Implications for the Sulfur Excess Paradox

Siyu Liu
Jilin University

Jian Lv
Jilin university https://orcid.org/0000-0002-6201-9888

Pengyue Gao
Jilin University

Andreas Hermann
University of Edinburgh https://orcid.org/0000-0002-8971-3933

Guochun Yang
Yanshan University

Yanchao Wang (wyc@calypso.cn)
Jilin University https://orcid.org/0000-0003-4518-925X

Yanming Ma
Jilin University https://orcid.org/0000-0003-3711-0011

Article

Keywords: sulfur excess, deep sulfur cycle

Posted Date: December 29th, 2020

DOI: https://doi.org/10.21203/rs.3.rs-125867/v1

Version of Record: A version of this preprint was published at Science Bulletin on January 1st, 2022. See the published version at https://doi.org/10.1016/j.scib.2022.01.005.

Stabilization of S_3O_4 at High Pressure-Implications for the Sulfur Excess Paradox

Siyu Liu,[1] Jian Lv,[1] Pengyue Gao,[1] Andreas Hermann,[2] Guochun Yang,[3] Yanchao Wang,[1,*] and Yanming Ma[1,4,†]

[1]*State key laboratory of superhard materials & International center of computational method and software, College of Physics, Jilin University, Changchun 130012, China*

[2]*Centre for Science at Extreme Conditions and SUPA, School of Physics and Astronomy, The University of Edinburgh, Edinburgh EH9 3FD, United Kingdom*

[3]*School of Science, Yanshan University, Qinhuangdao 066004, China*

[4]*International Center of Future Science, Jilin University, Changchun 130012, China*

(Dated: December 9, 2020)

The geological conundrum of "sulfur excess" refers to the finding that predicted amounts of sulfur, in the form of SO_2, discharged in volcanic eruptions much exceeds the sulfur available for degassing from the erupted magma. Exploring the source of the excess sulfur has been the subject of considerable interest. Here, from a systematic computational investigation of sulfur-oxygen compounds under pressure, a hitherto unknown S_3O_4 compound containing a mixture of sulfur oxidation states +II and +IV emerges and is predicted to be stabilized above a pressure of 79 GPa. We predict that S_3O_4 can be produced via multiple redox reactions involving subducted S-bearing minerals (e.g., sulfates and sulfides) at high pressure and temperature conditions relevant to the deep lower mantle, and conversely be decomposed into SO_2 and S at shallow depths of Earth. Therefore, S_3O_4 can be considered as a key intermediate compound to promote the decomposition of sulfates to release SO_2, which offers an alternative source of the excess sulfur released during explosive eruptions. These findings provide a possible resolution to the geological paradox of "excess sulfur degassing" and a viable mechanism for understanding of S exchange between Earth's surface and the lower mantle for the deep sulfur cycle.

PACS numbers:

Sulfur (S) is one of the major multi-valent volatile elements, broadly distributed throughout the Earth, and participating in a variety of fundamental geochemical processes (e.g., the global biochemical circulation [1], metal transport [2], atmospheric S loading during volcanic eruption and core–mantle segregation [3]). Generally, the chemical speciation of S is strongly influenced by a wide range of oxidation states available. Under highly reducing environments, S dominantly exhibits an oxidation state of -II as sulfide, whereas under strongly oxidizing conditions it shows an oxidation state of +VI in sulfate. Other chemical species where S takes up intermediate oxidation states such as in polysulfides, elemental S, sulfite, or thiosulfate sulfite may exist as well in different geochemical settings [2, 4, 5]. It happens often that the behavior of S in natural processes associated with complex oxidation-reduction reactions is unpredictable due to changes in the oxidation state of S across the range -II to +VI. Therefore, the geochemical behavior of S in the Earth is replete with paradoxes and there are many open questions in geochemical processes related to S-bearing minerals.

A well-known geological paradox called "sulfur excess degassing" has been evidenced at numerous subduction zone volcanoes [6, 7], where the amount of S (principally in the form of SO_2) released during explosive eruptions can be orders of magnitude larger than that estimated to degassing from the erupted melt [5]. A variety of sources for the excess S released by magmas in volcanic emission [8, 9] have been proposed: dissolution in the silicate liquid [10, 11] or a coexisting gas phase at depth before eruption [7, 12], gas expulsion from magma mixing [13, 14], crystallization-induced exsolution (second boiling) [15], or the breakdown of S-bearing minerals [16]. These mechanisms were proposed based on the magmatic systems, which are related to volcanic eruptions in a shallow crust. It should be noted, however, that the ultimate source of the S found near the Earth's surface is derived from the Earth's mantle [17].

Oxygen is one of the most abundant elements in Earth and has provided a critical control on the nature of Earth S reservoirs. The compounds formed by S and O have important implications for the geochemical processes and provide a critical control on the nature of Earth sulfur reservoirs. Thus, a key question that needs to be resolved regards formation and properties of S-O compounds under mantle conditions. Various S-O compounds such as SO [18], SO_2 [19], SO_3 [20], S_7O [21] and S_8O [22] have been proposed at ambient pressure. High pressure as characteristic for the mantle can drastically modify chemical properties of elements and promote the formation of unexpected minerals [23]. Currently, only SO_2 has been experimentally studied up to 60 GPa [24]. The other S-O compounds have been insufficiently understood at high pressures till now. A pressing task is to investigate the S-O compounds viable under pressure conditions relevant in Earth's mantle.

Here, we report an extensive exploration of the high-pressure phase diagrams of S-O compounds. Besides the known SO_2 and SO_3 compounds, an unexpected stoichiometry of S_3O_4 with an intriguing crystal structure, which contains a mixture of +II and +IV oxidation states of S, is predicted to appear at high pressure. We show that S_3O_4 is able to be produced in reactions of sulfates and sulfides with iron and goethite under high pressure and temperature (P-T) conditions in the deep mantle, and decompose into SO_2 and S at low P-T conditions relevant to shallow depths of Earth, thus offering insightful implications for S cycles and the

origin of excess S degassing observed in volcanic eruptions.

The crystal structure searches on S_xO_y (x=1-3, y=1-4) at the selected pressures of 50, 70 and 100 GPa have been performed using the swarm intelligence based-CALYPSO method [25–27], which has been successful in resolving crystal structures of a large number of materials at high pressure [28]. The maximum simulation cell of structure searches contains 40 atoms for each composition. Structural optimization, electronic structure and phonon calculations were performed in the framework of density functional theory within the generalized gradient approximation [29] as implemented in the VASP code [30]. The electron-ion interaction was described by the projector augmented-wave potentials [31], with $3s^2 3p^4$ and $2s^2 2p^4$ configurations treated as the valence electrons of S and O, respectively. A kinetic cutoff energy of 900 eV and a spacing of $2\pi\times0.03$ Å^{-1} for Monkhorst-Pack k-mesh sampling [32] were adopted to give well converged total energies (~1 meV/atom). The ionic positions were fully relaxed until the residual force acting on each ion was less than 1 meV/Å. Due to the layered structure of S_3O_4, influence of van der Waals interactions was considered using the optB88-vdW functional [33]. The dynamic stability of the predicted new phases was verified by phonon calculations using the direct supercell method as implemented in the PHONOPY code [34].

Our main structure searching results are depicted in the convex hull diagrams of Fig. 1(a). The energetic stabilities of a variety of S-O structures are evaluated from their formation enthalpies relative to the dissociation products of the relevant elemental S [35, 36] and O solids [37]. At 50 and 70 GPa, the known stoichiometries SO_2 and SO_3 are readily identified as stable in our structure searching simulations. At 100 GPa, an unexpected composition of S_3O_4 becomes stable with respective to the dissociation products of the elemental S and SO_3, whereas SO_2 cannot be stabilized any more.

The predicted stable pressure ranges for the considered structures are listed in Fig. 1(b). SO_3 is found to be the most stable phase against decomposition throughout the studied pressure range (50-100 GPa). A phase transition for SO_3 from the known α-phase to the predicted $R\bar{3}c$-phase is calculated to take place at 75 GPa. For SO_2, the pressure-induced phase transformation between molecular ($Pna2_1$) and polymeric structures ($Pmc2_1$) is identified at 17.5 GPa (Fig. S1). Note that the predicted high-pressure structure of $Pmc2_1$ (Fig. S1b) is isomorphic to the β-SeO_2 structure [38] that has recently been predicted in another study [24]. S_3O_4 is energetically favorable relative to decomposition into element S and SO_2 or SO_3 in the pressure range of 79-102 GPa (Fig. 1c). The emergence of S_3O_4 leads to the instability of SO_2 above 81.5 GPa. We calculated phonon dispersions and observed no imaginary frequencies for all the predicted structures discussed above (Fig. S2), indicating that these predicted structures are dynamically stable.

The α-phase of SO_3 is composed of oxygen-sharing

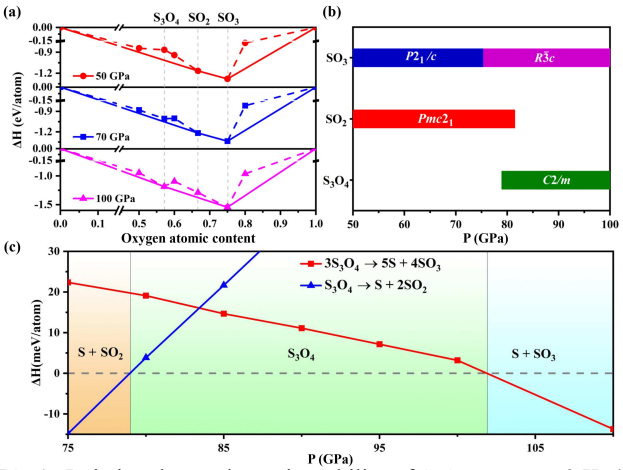

FIG. 1: Relative thermodynamic stability of S-O system at 0 K. (a) Convex Hull data of the $S_{1-x}O_x$ system at 50 GPa (top), 70 GPa (middle) and 100 GPa (bottom). The formation enthalpies ΔH for each structure were calculated with respect to elemental S and O solids by $\Delta H(S_{1-x}O_x)=H(S_{1-x}O_x)$-(1-x)H(S solid)-xH(O solid) (0<x<1). The known S-III [48], S-IV [49] and ϵ-O phases [51] were selected as the reference structures in the corresponding stable pressure ranges. The stable structures locate on the solid lines, while the metastable structures sit on the dashed lines. (b) Predicted pressure-composition phase diagram of S-O phases. (c) Calculated pressure-enthalpy diagram for the reactions $3S_3O_4 \rightarrow 4SO_3 + 5S$ and $S_3O_4 \rightarrow 2SO_2 + S$ using optB88-vdw functional. The zero-point energy was included in the above energy calculations.

SO4 tetrahedron chains and polymerizes into the predicted polymeric structure (space group $R\bar{3}c$, FeF_3 structure type), consisting of edge-sharing SO6 octahedra (Fig. 2a). The structure of S_3O_4 (Fig. 2b) is inherently layered, and contains mixed four-fold and six-fold coordination of S. Specifically, S1 is linearly coordinated to two O atoms, while S2 is square-coordinated to four O atoms. All S atoms are bonded to two adjacent S atoms, thus forming zigzag polymeric all-S chains. The S1-S1 and S1-S2 bond lengths are 2.22 and 2.13 Å at 80 GPa, respectively, slightly longer than the S-S bond lengths (2.01 Å) in S-III phase, therefore indicating relatively weaker covalent S–S bonding. To further decipher the nature of the bonding, we have examined the electron localization function (ELF) [39] of S_3O_4 in the (100) and (010) planes (Fig. 2c). Two inequivalent S atoms are clearly seen, while a less localized charge distribution is seen on the S–O bonds, indicating a significant degree of ionicity between the O anions and S cations. Clear covalent S-S bonding is evidenced by the strong charge localization between the nearest-neighbor S-S.

The oxidation states of S in geological environments play pivotal roles in deciding planetary chemical and physical dynamics [40]. Generally, the oxidation state in the crystal is closely related to the local coordination and charge transfer. The S oxidation states in SO_2 and SO_3 can be assigned unambiguously as +IV and +VI, respectively. In contrast, the two- and four-fold coordination of S atoms with O atoms in S_3O_4 reveals its mixed-valence state. A Bader charge analysis

[41], summarized in Table 1, corroborates this interpretation. While the Bader charges systematically underestimate the formal charge state (O^{2-} here has a charge -1.28e in the SO_2), they are consistent and strongly correlated. In SO_3, S has a formal charge state of +VI, and there is a charge transfer of 3.90e from S to O, very close to that in SF_6 (~3.73e). In SO_2, S has a formal charge state of +IV, the charge transfer is 2.56e. In S_3O_4, the partial charge of 2.68e in square coordinated S2 is almost equal to that in the SO_2 case, so that S2 can be considered as having an oxidation state of +IV. On the other hand, S1 is significantly less positively charged (1.04e) than the S anion in SO_2. This result highlights a crucial distinction of the S1 compared to S in SO_2, indicating that the linearly coordinated S1 in S_3O_4 adopts the rare +II S oxidation state.

TABLE I: Partial charges for various S-O compounds obtained from Bader integration at 80 GPa.

Compounds	S(e)		O(e)
	S1	S2	
S_3O_4	+1.04	+2.68	-1.19
SO_2	+2.56		-1.28
SO_3	+3.90		-1.30

The S-O compounds tend to be insulating, as satisfying the octet rule usually leads to opening of a band gap. This rule is applicable to the predicted polymeric phases of SO_2 and SO_3. However, in S_3O_4 two bands are found to cross the Fermi level, forming an electron pocket around the Z point and a hole pocket spanning the X and Y points (Fig. 2d), giving rise to a clear metallic character of S_3O_4. The projected density of states (Fig. 2d) shows that both O and the linearly coordinated S1 contribute to the density of electronic states at the Fermi level and the latter contribution is dominant. The metallic character originates from an overlap of the S1 electron lone pairs, which depends on interlayer distance (Fig. S3).

Since both the S and O are typical light elements, the stability of S-O compounds may be quite sensitive to temperature. To assess the viability at high temperature, we further examine their energetic and structural stability at relevant simultaneous high P-T conditions. The free energies including the vibrational contributions and entropic effects are evaluated for each phase using the quasi-harmonic approximation. The polymeric structure of SO_2 was found to be unstable with respect to SO_3 and S_3O_4 at 82 GPa and 0 K. The stability field of SO_2 with respect to S_3O_4 and SO_3 shifts towards higher pressures with increased temperature (Fig. 3a). The mechanism of decomposition of SO_2 into S_3O_4 and SO_3 is driven by the denser structural packing of S_3O_4 and SO_3 at high pressures. For example, the relative compression of $\Delta V/V$ for decomposition of SO_2 into S_3O_4 and SO_3 approaches at -10.6% at 80 GPa, where volumes of SO_2, S_3O_4 and SO_3 are 7.55, 7.41 and 6.17 Å^3 per unit,

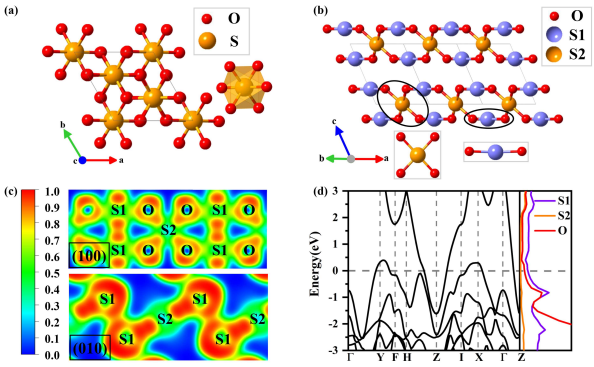

FIG. 2: (a) Crystal structure of $R\bar{3}c$ along the c-axis at 100 GPa. (b) Crystal structure of $C2/m$-S_3O_4 at 100 GPa. Calculated ELF (c) in (100) and (010) planes of $C2/m$-S_3O_4 at 80 GPa. (d) Band structures and the projected density of states (PDOS) of $C2/m$-S_3O_4 at 80 GPa. The dashed line indicates the Fermi level. The band structures are calculated using the Heyd–Scuseria–Ernzerhof hybrid functional [42, 43].

respectively. Formation enthalpy calculations further reveal that S_3O_4 is energetically favorable relative to decomposition into SO_3 and S above 70 GPa and that temperature has a minor impact on the threshold pressure (Fig. 3b). Against decomposition into SO_2 and S, the stability region of S_3O_4 is shifted to higher pressure with rising temperature, increasing from 79 GPa at 0K to 100 GPa at 2,300 K (Fig. 3c). Ab-initio molecular dynamics calculations show that S_3O_4 remains firmly solid at 2,000 K in the pressure range 80-100 GPa corresponding to deep mantle conditions (see Fig. S4), revealing that S_3O_4 may exist in solid form in the deep mantle. Overall, the predicted S_3O_4 is stable at P-T conditions relevant to Earth's lower mantle [44], but decompose into SO_2 and S at low pressure.

It is well-known that the exchange of S between Earth's surface and the mantle, i.e., transporting S to the mantle via subduction and returning it to the surface by volcanic degassing, results in a global S cycle [45]. Previous studies have indicated that sulfates (e.g., $CaSO_4$ and $MgSO_4$) are transported into the deep Earth's mantle [45, 46], where an estimated ~1 weight % metallic Fe is present due to self-reduction reactions at high-pressure [47]. Thus, we explore the possibility for production of S_3O_4 by decomposition of sulfates ($CaSO_4$/$MgSO_4$) using Fe as a reducing agent. The following decomposition routes are examined in Earth's mantle pressure conditions:

$$3CaSO_4 + 5Fe \rightarrow 3CaO + 5FeO + S_3O_4, \quad (1)$$

$$3MgSO_4 + 5Fe \rightarrow 3MgO + 5FeO + S_3O_4. \quad (2)$$

The calculated negative reaction enthalpies (Δ H, see Fig. 4a) support the decomposition of sulfates into S_3O_4 at high pressure. For the route in Equation (1), the decomposition takes place above 75 GPa, while the reaction described in Equation (2) occurs in the entire considered range of pressures

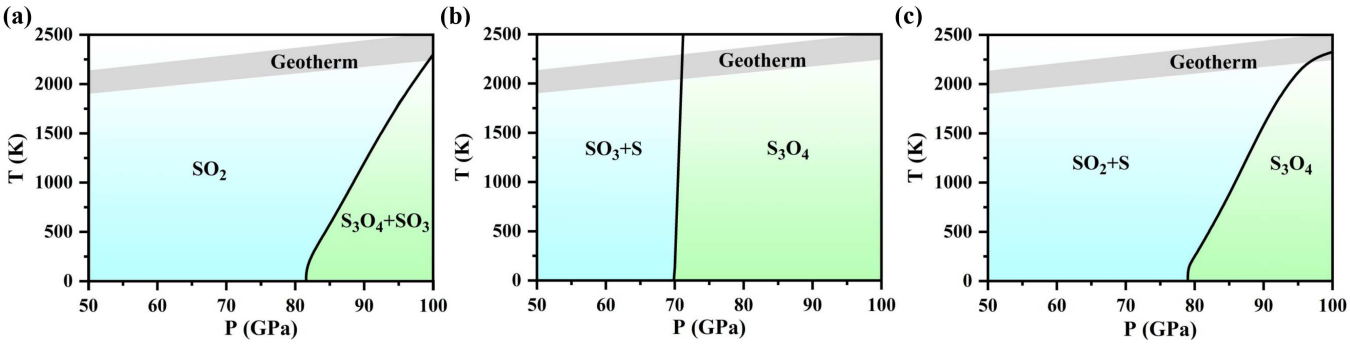

FIG. 3: The P-T phase diagrams for the reactions of $5SO_2 \rightarrow S_3O_4 + 2SO_3$ (a), $4SO_3 + 5S \rightarrow 3S_3O_4$ (b) and $2SO_2 + S \rightarrow S_3O_4$ (c). The geotherm curve is adapted from Ref. [44].

from 70 GPa to 100 GPa. Furthermore, we also explore the oxidation reactions of sulfides (e.g., FeS and FeS_2, a small amount of which is believed to be present in Earth's mantle [48, 49]) with FeOOH that acts as oxidizing agent to produce S_3O_4 following the routes defined by Equations (3) and (4). It is seen from Fig. 4a that these defined reactions can indeed take place at the pressures relevant to the deep mantle.

$$3FeS_2 + 22FeOOH \rightarrow 11H_2O + 25FeO + 2S_3O_4, \quad (3)$$

$$3FeS + 14FeOOH \rightarrow 7H_2O + 17FeO + S_3O_4. \quad (4)$$

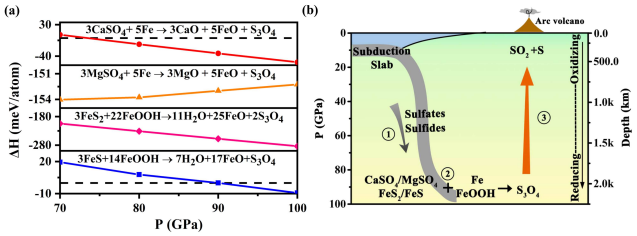

FIG. 4: (a) Relative enthalpy of proposed reactions forming S_3O_4 at high pressure. (b) The proposed processes for exchange of S between Earth's surface and mantle.

According to our results, three possible processes can occur for the sulfur cycle in the Earth (Fig. 4b). Firstly, the S-carrying sulfates or sulfides (e.g., $CaSO_4$, FeS_2 [50], and FeS [51]) are transported to the deep mantle within subduction slabs. Then they can react with Fe or FeOOH (minerals present in Earth's mantle) to produce S_3O_4 at reducing or oxidizing conditions. If S_3O_4 formed in the deep mantle ascends, by mantle dynamic processes, to shallow depths of Earth and low pressure conditions, it would decompose into S and SO_2, which is the principal form of S released during explosive eruptions (Fig. 3c). While the mechanism of direct decomposition of S-bearing minerals (e.g., $CaSO_4$, FeS_2, and FeS) to release SO_2 as an explanation of "sulfur excess" paradox is not supported even at high pressure [11] (see Fig. S5 for enthalpy calculations), the present compound S_3O_4, which was not previously considered, provides an alternative sulfur reservoir in the deep mantle, completes the deep sulfur cycle and helps to explain the paradox of "sulfur excess" in volcanic eruptions.

In summary, a hitherto unknown compound S_3O_4 has been identified to become stable at high P-T conditions relevant to the deep mantle. It contains a mixture of S(II) and S(IV) oxidation states and exhibits a peculiar metallic nature. A systematic examination of relevant formation and decomposition reactions reveals that S_3O_4 might be considered as a key ingredient to promote redox reactions of sulfate or sulfide in the deep mantle and to release SO_2 at shallow depths of Earth, thereby offering insightful implication on the origin of excess S degassing observed in volcanic eruptions. The present results have fundamental significance and implications for practical processes in chemistry and geoscience and further experimental exploration is highly expected.

This research was supported by the National Key Research and Development Program of China under Grant No. 2016YFB0201201; the National Natural Science Foundation of China under Grants No. 11404128, 11822404, 11534003 and 21873017; Program for JLU Science and Technology Innovative Research Team; and the Science Challenge Project, No. TZ2016001. Part of the calculation was performed in the high-performance computing center of Jilin University.

S.L. and J.L. contributed equally to this work.

* Electronic address: wyc@calypso.cn
† Electronic address: mym@jlu.edu.cn

[1] R. Steudel, in *Elemental Sulfur und Sulfur-Rich Compounds II* (Springer, 2003), pp. 203–230.
[2] G. S. Pokrovski and L. S. Dubrovinsky, Science **331**, 1052 (2011).
[3] Z. Wang and H. Becker, Nature **499**, 328 (2013).
[4] G. Barré, L. Truche, E. F. Bazarkina, R. Michels, and J. Dubessy, Chem. Geol. **462**, 1 (2017).
[5] H. Keppler, Science **284**, 1652 (1999).
[6] P. J. Wallace and T. M. Gerlach, Science **265**, 497 (1994).
[7] H. Shinohara, Rev. Geophys. **46**, RG4005 (2008).
[8] P. J. Wallace and M. Edmonds, Rev. Mineral. Geochem. **73**, 215 (2011).

[9] M. Edmonds and A. W. Woods, J. Volcanol. Geoth. Res. **368**, 13 (2018).
[10] H. Keppler, Geochim. Cosmochim. Ac. **74**, 645 (2010).
[11] M. Masotta, H. Keppler, and A. Chaudhari, Geochim. Cosmochim. Ac. **176**, 26 (2016).
[12] M. B. Lierenfeld, Z. Zajacz, O. Bachmann, and P. Ulmer, Geochim. Cosmochim. Ac. **226**, 50 (2018).
[13] M. Edmonds, A. Aiuppa, M. Humphreys, R. Moretti, G. Giudice, R. Martin, R. Herd, and T. Christopher, Geochem., Geophy., Geosy. **11** (2010).
[14] V. Kress, Nature **389**, 591 (1997).
[15] Y. Su, C. Huber, O. Bachmann, Z. Zajacz, H. Wright, and J. Vazquez, J. Geophys. Res-Sol. Ea. **121**, 5624 (2016).
[16] J. Devine, H. Sigurdsson, A. Davis, and S. Self, J. Geophys. Res-Sol. Ea. **89**, 6309 (1984).
[17] J.-L. Li, E. M. Schwarzenbach, T. John, J. J. Ague, F. Huang, J. Gao, R. Klemd, M. J. Whitehouse, and X.-S. Wang, Nat. Commun. **11**, 1 (2020).
[18] B. N. Frandsen, P. O. Wennberg, and H. G. Kjaergaard, Geophys. Res. Lett. **43**, 11 (2016).
[19] B. Post, R. Schwartz, and I. Fankuchen, Acta Crystallogr. **5**, 372 (1952).
[20] R. Westrik and C. MacGillavry, Acta Crystallogr. **7**, 764 (1954).
[21] R. Steudel, R. Reinhardt, and T. Sandow, Angew. Chem. Int. Ed. English **16**, 716 (1977).
[22] P. Luger, H. Bradaczek, R. Steudal, and M. Rebsch, Chem. Ber. **109**, 180 (1976).
[23] Q. Hu, D. Y. Kim, W. Yang, L. Yang, Y. Meng, L. Zhang, and H.-K. Mao, Nature **534**, 241 (2016).
[24] H. Zhang, O. Tóth, X.-D. Liu, R. Bini, E. Gregoryanz, P. Dalladay-Simpson, S. De Panfilis, M. Santoro, F. A. Gorelli, and R. Martoňák, Proc. Natl. Acad. Sci. **117**, 8736 (2020).
[25] Y. Wang, J. Lv, L. Zhu, and Y. Ma, Phys. Rev. B **82**, 094116 (2010).
[26] Y. Wang, J. Lv, L. Zhu, and Y. Ma, Comput. Phys. Commun. **183**, 2063 (2012).
[27] B. Gao, P. Gao, S. Lu, J. Lv, Y. Wang, and Y. Ma, Sci. Bull. **64**, 301 (2019).
[28] Y. Wang and Y. Ma, J. Chem. Phys. **140**, 040901 (2014).
[29] J. P. Perdew, K. Burke, and M. Ernzerhof, Phys. Rev. Lett. **77**, 3865 (1996).
[30] G. Kresse and J. Furthmüller, Phys. Rev. B **54**, 11169 (1996).
[31] P. E. Blöchl, Phys. Rev. B **50**, 17953 (1994).
[32] H. J. Monkhorst and J. D. Pack, Phys. Rev. B **13**, 5188 (1976).
[33] J. Klimeš, D. R. Bowler, and A. Michaelides, Phys. Rev. B **83**, 195131 (2011).
[34] A. Togo, F. Oba, and I. Tanaka, Phys. Rev. B **78**, 134106 (2008).
[35] O. Degtyareva, E. Gregoryanz, M. Somayazulu, P. Dera, H.-K. Mao, and R. J. Hemley, Nat. Mater. **4**, 152 (2005).
[36] C. Hejny, L. Lundegaard, S. Falconi, M. McMahon, and M. Hanfland, Phys. Rev. B **71**, 020101 (2005).
[37] H. Fujihisa, Y. Akahama, H. Kawamura, Y. Ohishi, O. Shimomura, H. Yamawaki, M. Sakashita, Y. Gotoh, S. Takeya, and K. Honda, Phys. Rev. Lett. **97**, 085503 (2006).
[38] D. Orosel, O. Leynaud, P. Balog, and M. Jansen, J. Solid State Chem. **177**, 1631 (2004).
[39] A. Savin, R. Nesper, S. Wengert, and T. F. Fässler, Angew. Chem. Int. Ed. English **36**, 1808 (1997).
[40] V. Stagno, D. O. Ojwang, C. A. McCammon, and D. J. Frost, Nature **493**, 84 (2013).
[41] R. F. Bader, Chem. Rev. **91**, 893 (1991).
[42] J. Heyd, G. E. Scuseria, and M. Ernzerhof, J. Chem. Phys. **118**, 8207 (2003).
[43] J. Paier, M. Marsman, K. Hummer, G. Kresse, I. C. Gerber, and J. G. Ángyán, J. Chem. Phys. **124**, 154709 (2006).
[44] R. Nomura, K. Hirose, K. Uesugi, Y. Ohishi, A. Tsuchiyama, A. Miyake, and Y. Ueno, Science **343**, 522 (2014).
[45] S. Jégo and R. Dasgupta, J. Petrol. **55**, 1019 (2014).
[46] A. R. Thomson, M. J. Walter, S. C. Kohn, and R. A. Brooker, Nature **529**, 76 (2016).
[47] D. J. Frost, C. Liebske, F. Langenhorst, C. A. McCammon, R. G. Trønnes, and D. C. Rubie, Nature **428**, 409 (2004).
[48] E. M. Smith, S. B. Shirey, S. H. Richardson, F. Nestola, E. S. Bullock, J. Wang, and W. Wang, Nature **560**, 84 (2018).
[49] E. M. Smith, S. B. Shirey, F. Nestola, E. S. Bullock, J. Wang, S. H. Richardson, and W. Wang, Science **354**, 1403 (2016).
[50] Y. V. Bataleva, Y. N. Palyanov, Y. M. Borzdov, and N. V. Sobolev, Geology **44**, 271 (2016).
[51] G. Prouteau and B. Scaillet, J. Petrol. **54**, 183 (2013).

Figures

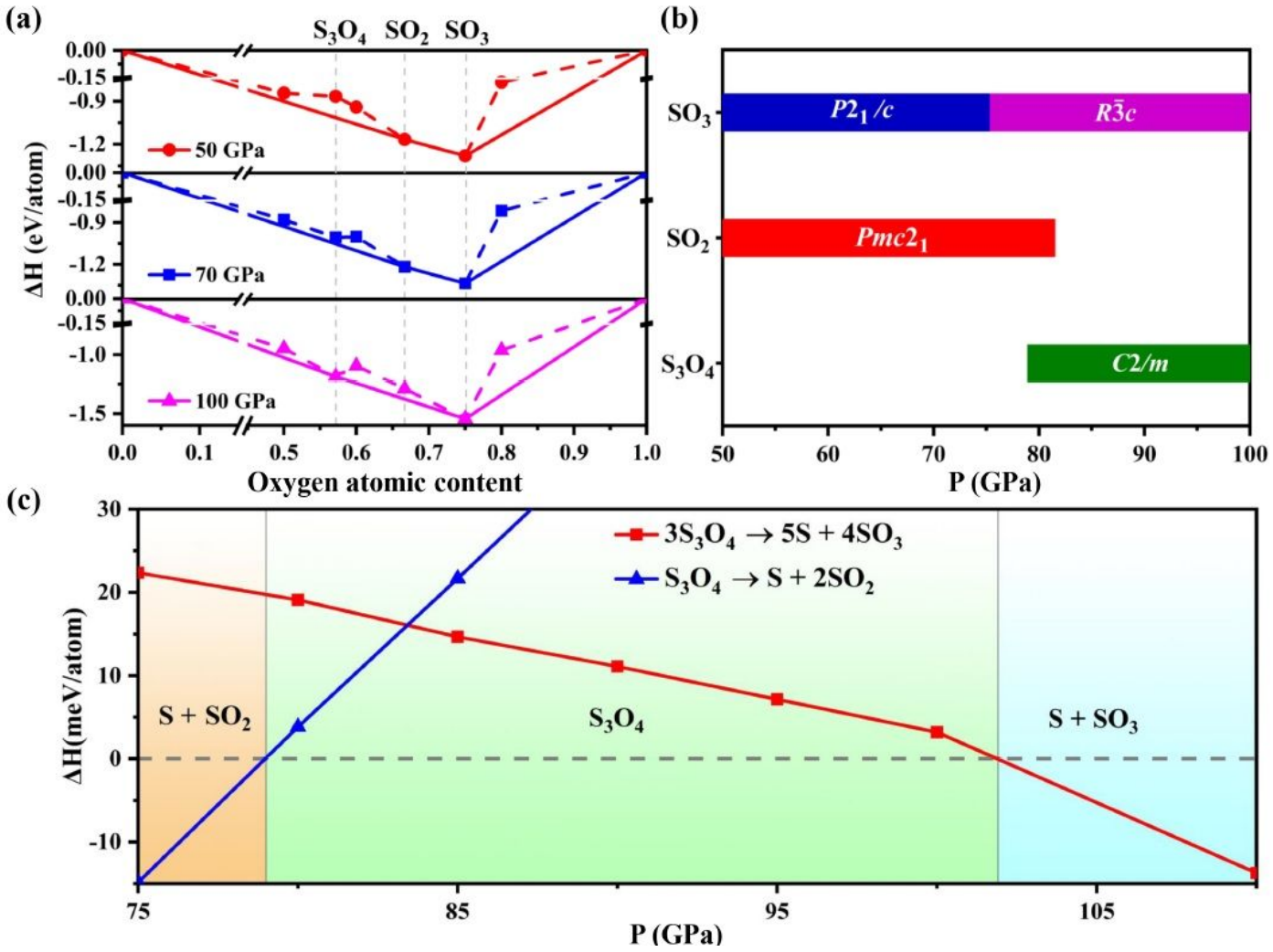

Figure 1

Relative thermodynamic stability of SO system at 0 K. (a) Convex Hull data of the S1−xOx system at 50 GPa (top), 70 GPa (middle) and 100 GPa (bottom). The formation enthalpies ΔH for each structure were calculated with respect to elemental S and O solids by ΔH(S1−x Ox)=H(S1−x Ox)(1x) H(S solid)xH(O solid) (0

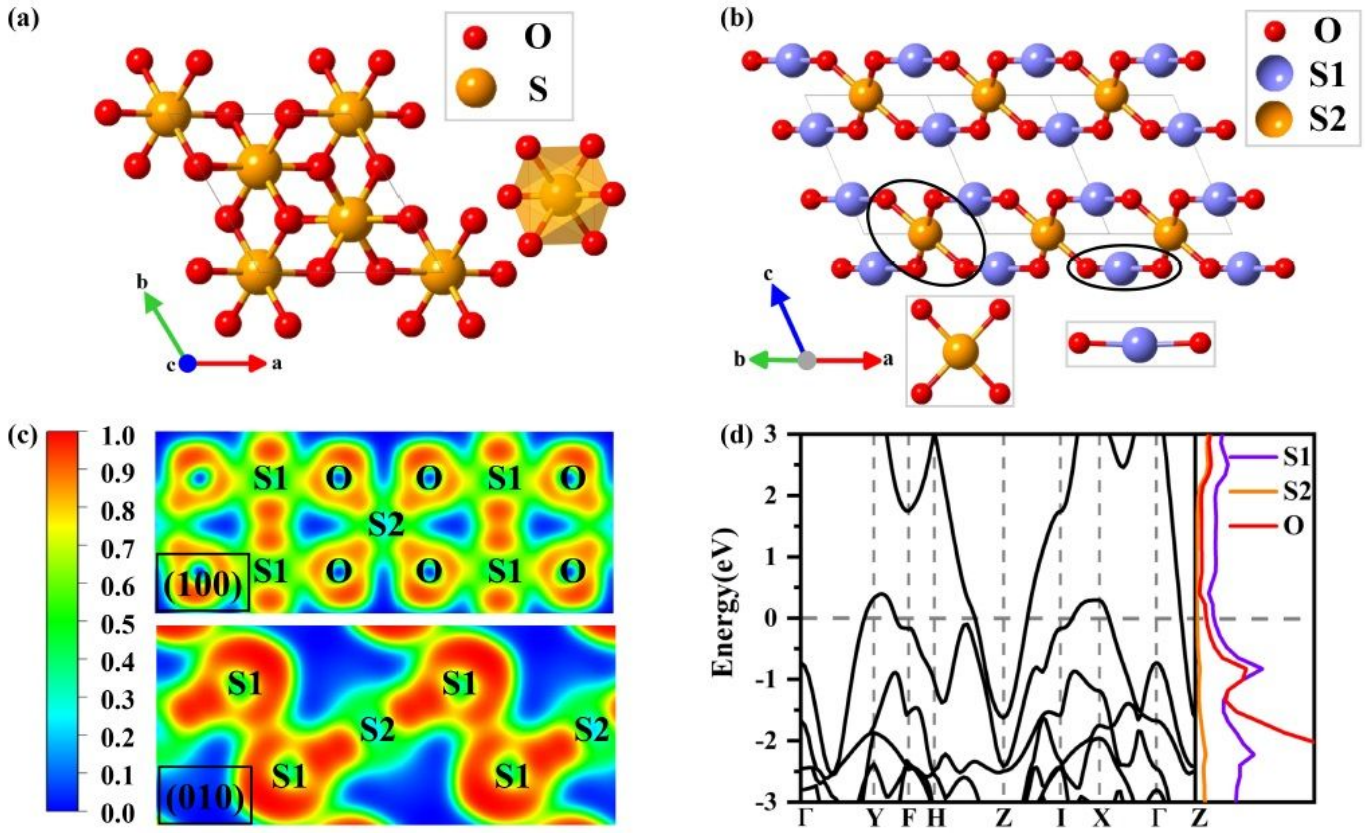

Figure 2

(a) Crystal structure of R3c along the caxis at 100 GPa. (b) Crystal structure of C2/mS3O4 at 100 GPa. Calculated ELF (c) in (100) and (010) planes of C2/mS3O4 at 80 GPa. (d) Band structures and the projected density of states (PDOS) of C2/mS3O4 at 80 GPa. The dashed line indicates the Fermi level. The band structures are calculated using the Heyd–Scuseria–Ernzerhof hybrid functional [42,43].

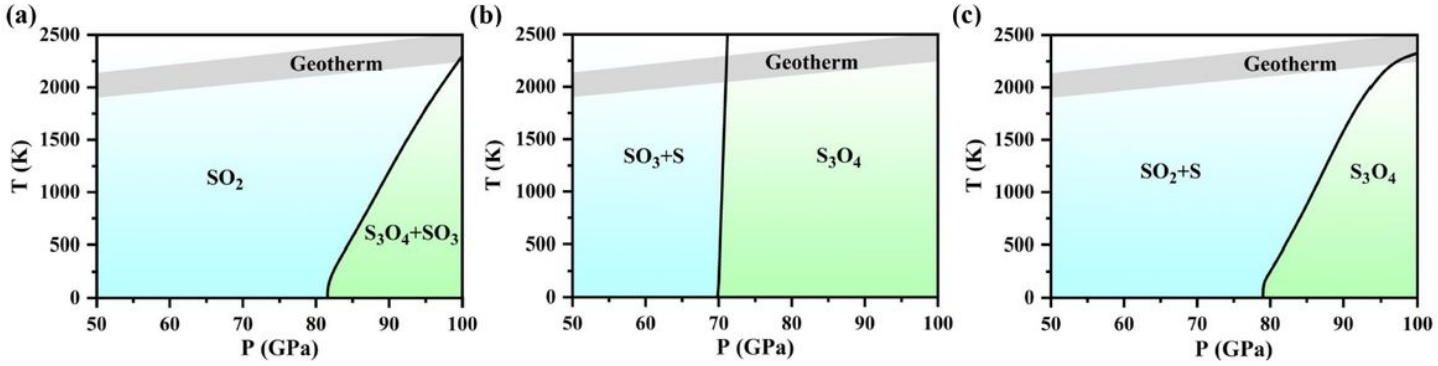

Figure 3

The PT phase diagrams for the reactions of 5SO2⟶S3O4+2SO3 (a), 4SO3+5S⟶3S3O4 (b) and 2SO2+S⟶S3O4 (c). The geotherm curve is adapted from Ref. [44].

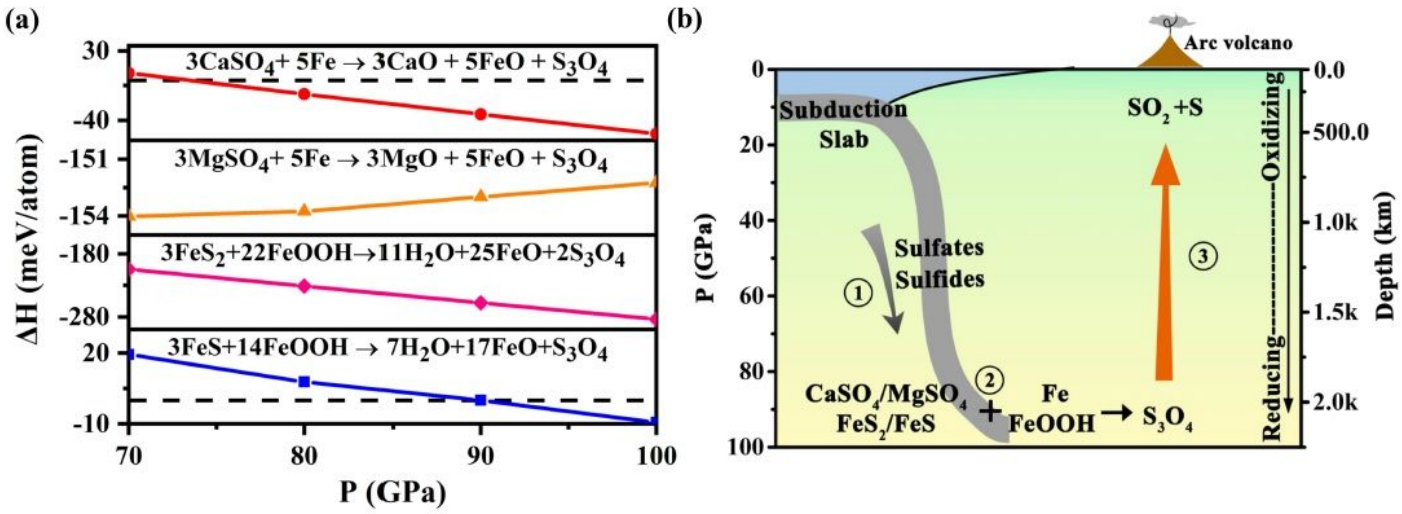

Figure 4

(a) Relative enthalpy of proposed reactions forming S3O4 at high pressure. (b) The proposed processes for exchange of S between Earth's surface and mantle.

Supplementary Files

This is a list of supplementary files associated with this preprint. Click to download.

- SupplementalMaterial.docx